International Journal of High-Rise Buildings
June 2020, Vol 9, No 2, 187-195
https://doi.org/10.21022/IJHRB.2020.9.2.187

International Journal of
High-Rise Buildings
www.ctbuh-korea.org/ijhrb/index.php

Structural Characteristics of Preloaded Deep Deck Composite Slabs with Tenns

Tae-Hun Lee[1], Jae-Hwan Kyung[2], Jong-Wook Song[2], and Sung-Mo Choi[3,†]

[1]*Master Course, Department of Architectural Engineering, University of Seoul, Republic of Korea*
[2]*Doctor Course, Department of Architectural Engineering, University of Seoul, Republic of Korea*
[3]*Professor, Department of Architectural Engineering, University of Seoul, Republic of Korea*

Abstract

As deep decks are commonly used in construction fields and high-rise building. etc, the slim floor system is increasingly employed. But, the drawback of the slim floor system is that the use of 250 mm deep decks in a structure having a clear span of more than 6 m because of deflection and flexural buckling. This study suggests a non-support construction method where tendons are installed in the deep decks of the slim floor structure to introduce preload in order to control deflection in a structure having a clear span of 9 m. Loading tests were conducted to verify the composite effect and flexural capacity of the preloaded deep deck composite slab and evaluate the serviceability of the supportless construction method. The results showed the complete composite behavior of the preloaded deep deck composite slab with tendons. The specimens satisfied deflection limit and the working load was approximately 25% of the maximum load capacity. It is deemed that the cross-sectional area and yield strength of the deck plate should be taken into account in slab design and the yield strength and diameter of the tendon should be determined with the pre-tension taken into consideration.

Keywords: Deep Deck, 250 mm Depth, Composite Slab, Pre-load Tendon

1. Introduction

The slim floor system shown in Figure 1 is increasingly employed due to the demand for the use of deep decks in construction fields and the increase of large and high-rise buildings. However, it is required to install temporary supports to deal with deflection and flexural buckling if the slim floor system where 250 mm or deeper decks are used is employed to a structure having a clear span of 6 m or longer. This study suggests installing tendons to apply preloads to the deep decks in order to control deflection in a structure having a clear span of 9 m. The preloaded tendons installed in the deep decks form cambers and act as flexural reinforcing bars after the concrete hardens. The deck plates of the composite slab not only act as molds but also resist stress. The composite effect and flexural capacity of the preloaded deep deck composite slab were tested and its serviceability was evaluated in this study.

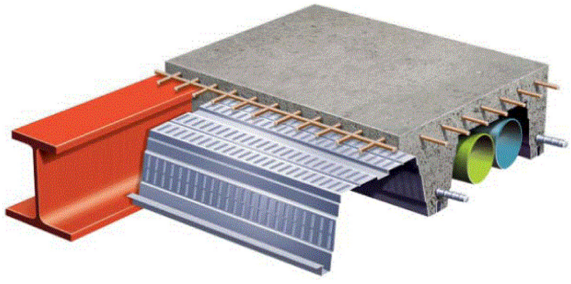


Fig. 1. Slim Floor System.

†Corresponding author: Sung-Mo Choi
Tel: +82-2-6490-2759, Fax: +82-2-6490-2749
E-mail: smc@uos.ac.kr

2. Composition and Structural Characteristics of Preloaded Deep Deck Composite Slab

2.1. Composition and Construction

Tendons are installed in the deep decks and preloads are applied to the tendons in order to form cambers. The deep decks deal with tensile force after the concrete hardens

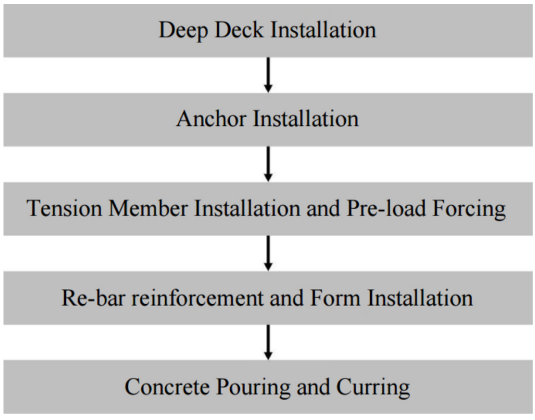


Fig. 2. Construction Process of Deep Deck Composite Slab.



Fig. 3. Fabrication of Deep Deck Composite Slabs with Pre-load Tendon.

and before loads are applied. Stress consumed for the pre-tension exerts influence on the floor structure. Since the tendons act as flexural reinforcing bars after the concrete hardens, the strain of the tendons decreases. But, it is restored by the pre-tension. Therefore, tension-dominated cross-sections can be designed to induce ductile behavior. Figure 2 and Figure 3 show the construction process of preloaded deep deck composite slab.

2.2. Characteristics of Floor Structure After Concrete Hardening

The characteristics of the floor structure after concrete hardening is classified into three types: 1) Complete composite behavior of the deep deck and the concrete, 2) Separation of the deep deck and the concrete, and 3)

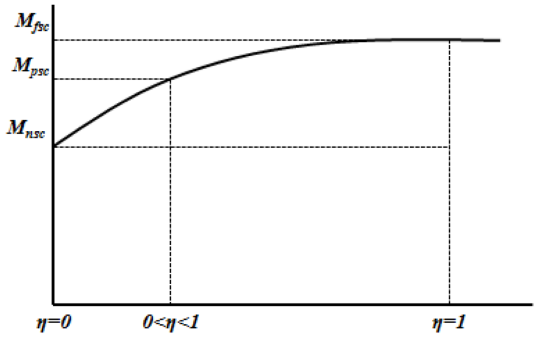


Fig. 4. Composition Degree Evaluation Method.

Partial composite behavior of the deep deck and the concrete. If the deep deck and the concrete show complete composite behavior, the load capacity of the floor structure is the greatest (M_{fsc}). In a non-composite slab, the concrete and the deck plate show compressive behavior and tensile behavior with the neutral axis acting as the imaginary dividing line as shown in Figure 5 (b). Most of the floor structures using the deck plates show partial composite behavior. Therefore, the maximum load capacity of the floor structure falls between complete composite moment and non-composite moment as shown in Figure 4, which determines the degree of composition.

$$M_{fsc}=C_C\left(c_{fsc}-\frac{a}{2}\right)+A_sF_u(cfsc-\overline{y_s})+A_{sr}F_{ur}(C_{fsc}-\overline{y_{sr}}) \quad \text{(Formula 1)}$$

$$M_{nsc}=C_C\left(d-\frac{a}{2}\right)+S_sF_{ur} \quad \text{(Formula 2)}$$

M_{fsc} : Complete Composite Flexural Load (Plastic Moment) (kN·m)

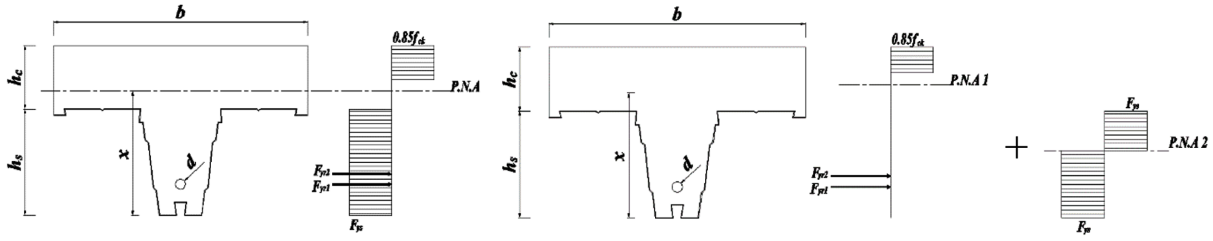
M_{nsc} : Partial Composite Flexural Load (kN·m)

M_{psc} : Non-composite Flexural Load (kN·m)

C_c : Concrete Compressive Strength (MPa)

A_s : Area of Deck Plate (mm^2)

A_{sr} : Area of Rebar (mm^2)



(a) Complete Composite Slab **(b) Non-composite Slab**

Fig. 5. Concept of Complete Composite/Non-composite Slab.

M_{fsc} : Complete Composite Flexural Load (Plastic Moment) (kN·m)
M_{nsc} : Partial Composite Flexural Load (kN·m)
M_{psc} : Non-composite Flexural Load (kN·m)
C_c : Concrete Compressive Strength (MPa)
A_s : Area of Deck Plate (mm^2)
A_{sr} : Area of Rebar (mm^2)
c_{fsc} : Plastic Neutral Axis of Complete Composite Section (mm)
y_i : Location of each Material (mm)
a : Equivalent Stress Block Depth (mm)
d : Effective Depth (mm)
F_y : Deck Plate Yield Strength (MPa)
F_{ur} : Rebar Yield Strength (MPa)
S_s : Deck Plate Elastic Section Coefficient

2.3. Complete Composite Floor Structure

If the deck plate and the concrete show complete composite behavior, the strain of the deck plate and that of the concrete have linear relationship with the neutral axis of the slab being the center as shown in Figure 6. The curvature of the slab and the strain values of the concrete and the deck plate can be calculated by Formula 3 and Formula 4, respectively, which estimate the structural behavior and the load - displacement relationship of the deflected member as shown in Figure 7. The load-displacement relationship can be classified into four phases. The lower part of the deck plate yields at point A, the tendon yields at point B, the total cross-section of the deck plate deforms plastically at point C and the upper part of the concrete reaches compressive strain at point D.

$$\rho=\delta^2+\left(\frac{l}{2}\right)^2 \quad \text{(Formula 3)}$$

$$\rho=\frac{y}{\rho} \quad \text{(Formula 4)}$$

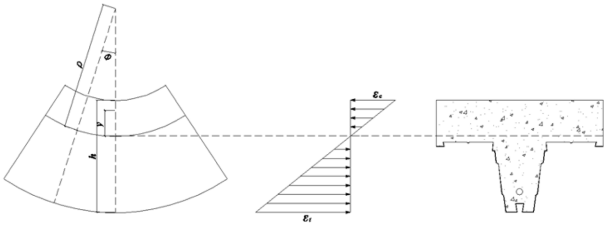


Fig. 6. Strain Variation of Complete Composite Member.

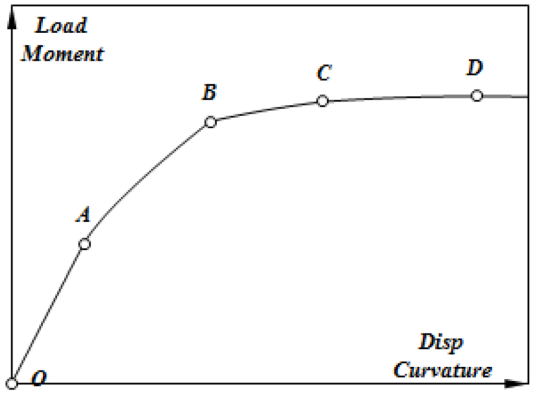


Fig. 7. Structural Behavior of Composite Slab.

2.4. Effect of Pre-tension on Floor Structre

If pre-tension is not applied, the strain of the tendon at the maximum load capacity of the slab is ⓐ in Figure 8 and the stress increases as the strain increases. At the early stage of introducing pre-tension, the strain of the tendon is ε_{pr}. When the maximum load capacity is reached after the concrete hardens, the strain of the tendon is ⓑ, which equals ⓐ plus ε_{pr}. The overall strain of the tendon increases, while its load capacity decreases because of the stress consumed for the pre-tension. The preloaded tendon undergoes deformation and yields earlier than that to which pre-tension is not applied. The cross-sections of the preloaded tendon become tension-dominated and the ductility increases.

3. Deep Deck Composite Slab Loading Test

3.1. Test Plan

In order to evaluate the flexural capacity of the composite slab with preloaded tendons suggested to control

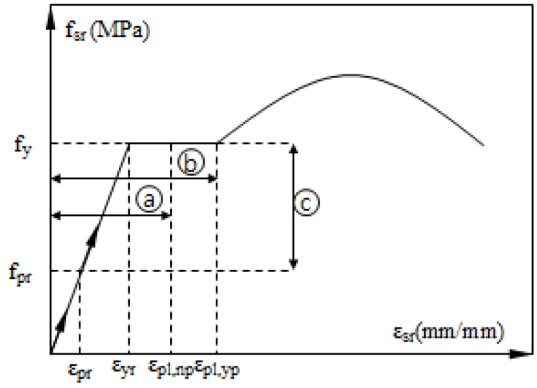


Fig. 8. Tension Residual Stress.

Table 1. Specimen List

Specimen	Camber (mm)	Pre-load (kN)	Rebar
FC01	0	0	
FC02	29.2	92.21(1.0)	
FC03	29.7	92.21(1.0)	Additional
FC04	22.8	73.06(0.8)	Additional
FC05	36.2	110.65(1.2)	Additional

Criteria Specimen: FC03

the deflection when employed in a long-span structure, specimens were fabricated and 2-point loading tests were conducted. Pre-tension and additional re-bar were chosen as variables to investigate structural behavior after concrete hardening and the influence of composite effect of the concrete and the deck on the steel ratio. Table 1 shows the specimen details.

3.2. Estimated Load Capacity

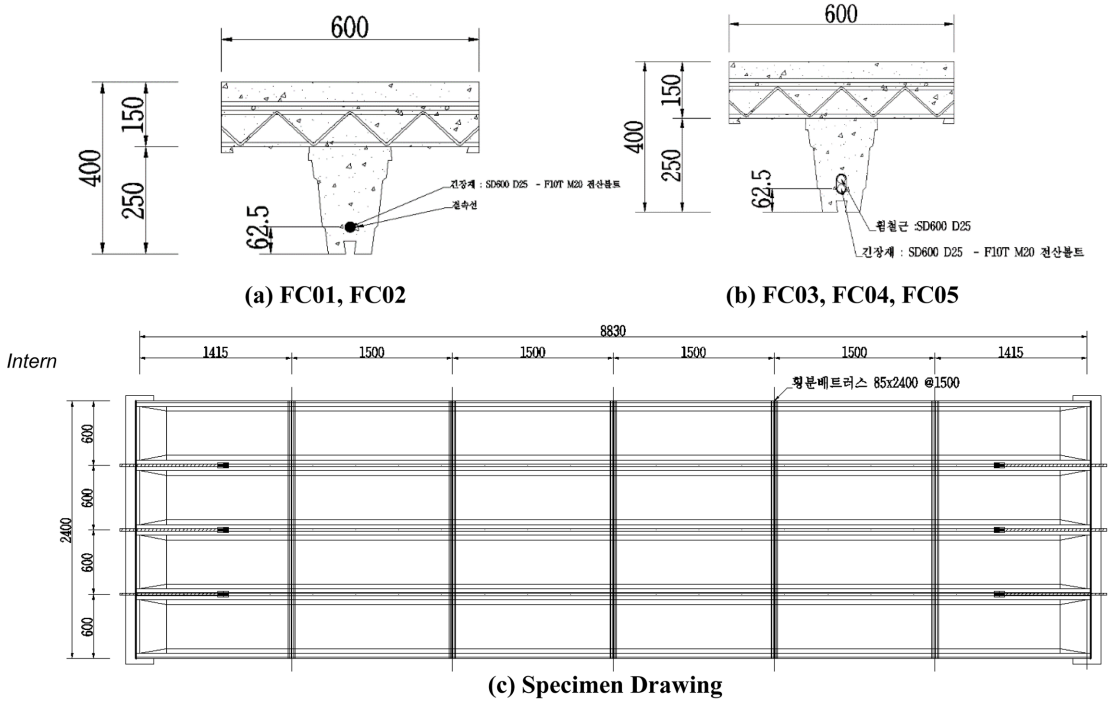
The load capacity of the specimens was calculated on the assumption that they were T-shaped simple beams. The deep decks were assumed to be integrated to the concrete at the centers of the cross-sections to act as tension members. Formulas 1~4 were used to calculate the estimated load of the specimens with their composite/ non-composite behaviors taken into consideration. Table 2 shows the estimated loads.

Table 2. Expected Specimen Maximum Load

Specimen	FC01, FC02(kN)	FC03, FC04, FC05(kN)
P_{max}	111.3	150.2
P_u	77.2	111
δ_c	72	90.5
P_{max} / P_u	1.44	1.35
K	1.29	1.51

3.3. Specimen Details and Test Method

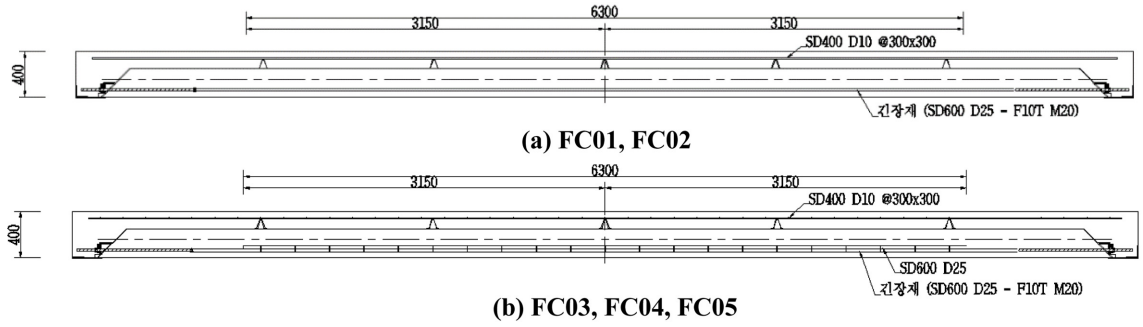
The deep decks were 8,830 mm in length and 1.4 mm in thickness. The topping concrete was 150 mm thick. D10 bars were arranged at the top of the decks at an interval of 200 mm as shown in Figure 9. Flexural reinforcing bars placed in specimens FC03, FC04 and FC05 were D23-SD600 and so were the tendons. Figure 10 shows the arrangement of the steel bars.



(a) FC01, FC02 (b) FC03, FC04, FC05

(c) Specimen Drawing

Fig. 9. Specimen Figure.



(a) FC01, FC02

(b) FC03, FC04, FC05

Fig. 10. Steel bar Details.

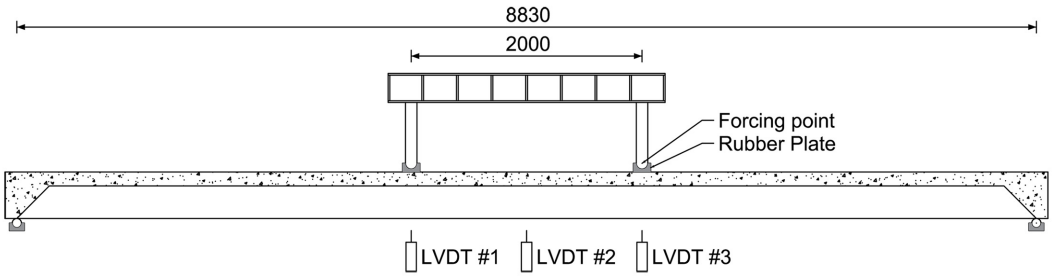


Fig. 11. Displacement Measurement Sensor Location.

A 3000 kN universal test machine was used for monotonic loading. The end of the specimen was hinged for 2-point loading at an interval of 2,000 mm. Strain gauges were placed at the top of the deck plate and LVDTs were placed at the center of the specimen and below the loading points. Figure 11 shows the location of the LVDTs to measure the deflection of the specimen.

3.4. Load-displacement relationship

Figure 12 shows load - displacement (P-Δ) relationships obtained from the tests and Figure 13 illustrates how yield load, yield displacement, ductility and initial stiffness are defined. Initial stiffness is defined as the slope of line ⓐ which starts from the origin of the P-Δ curve and touches it at 1/3 of maximum load capacity. Yield load is load at the point of intersection between line ⓐ and line ⓒ. Yield displacement is defined as displacement at yield load on the P-Δ curve. The slope of line ⓑ is 1/3 of line ⓐ. Line ⓒ is tangential to the P-Δ curve and parallel to line ⓑ. Ductility is defined as the ratio of displacement at 0.8 P_{max} after the maximum load to yield displacement.

As shown in table 3 summarizing the results, the stiffness and displacement of the specimens varied depending on the steel ratio.

3.5. Failure Mode

Specimen FC01 underwent the compressive failure of the concrete at its center after the maximum load. Cracks

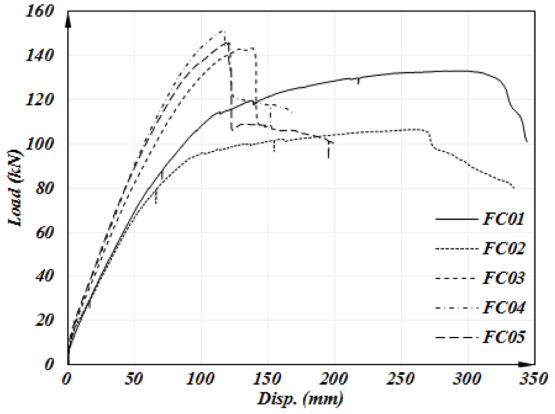


Fig. 12. Load-displacement Graph.

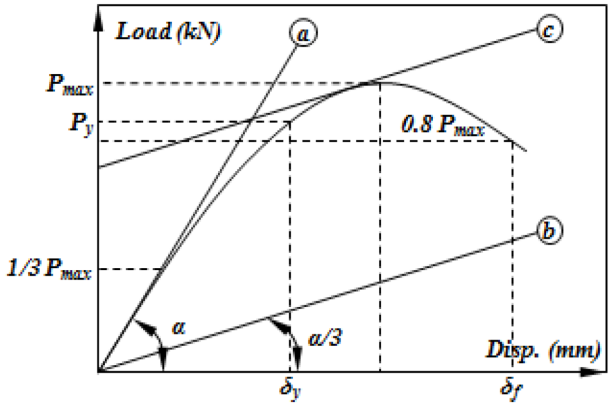


Fig. 13. Yield Point Decision Method.

Table 3. Experiment Result

	FC01	FC02	FC03	FC04	FC05
P_u (kN)	81	66	97.5	112.5	100.5
$P_{max,\ell}$ (kN)	132.95	105.97	143.05	151.35	145.78
$P_{max,c}$ (kN)	111.3	111.3	150.2	150.2	150.0
δ_c (mm)	62.02	48.9	62.73	66.53	58.42
δ_f (mm)	309.10	297.13	140.50	123.95	122.04
P_{max}/P_u	1.64	1.61	1.47	1.35	1.45
δ_f/δ_u	4.98	6.08	6.24	1.86	2.09
K (kN/mm)	1.61	1.68	1.96	2.08	2.18

$P_{max,\ell}$: 2 Point Load corresponding to M_{fsc} (Complete Composite Moment)

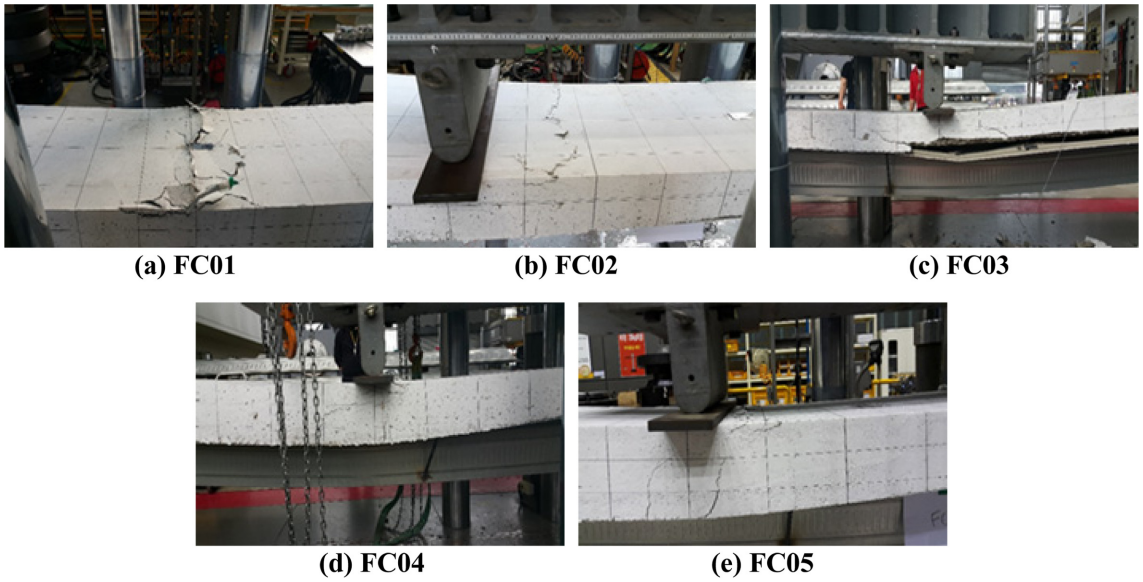


Fig. 14. Failure Mode.

were observed at one of the two loading points of the other specimens. Figure 14 shows the failure mode of the specimens.

4. Analysis & Implication

4.1. Composite Effect

The plastic moment of the specimens was calculated on the premise of complete compositeness and the degree of compositeness was determined by the comparison of complete composite moment and ultimate moment. The estimated complete composite moment, non-composite moment and concrete slab moment of the specimens are shown in Table 4. The ratio of ultimate moment to complete composite moment is approximately 1 in all of the specimens, verifying complete compositeness. Therefore, the fact that the deck plates resist stress should be considered when the load capacity of the deep deck composite slab with preloaded tendons is calculated.

4.2. Deflection and load capacity

Table 6 summarizes the deflection, deflection ratio, load ratio and strength of the specimens. Dead load and live load values provided in 0303.2.1 Basic Uniform Live Load in the KBC 2009 shown in table 5 were used. Deflection caused by working load was less than deflection limit (L/360 = 25 mm) in all of the specimens. The ratio of working load deflection to deflection limit ranged between 0.35 and 0.55. Coefficient load was approximately 25% of maximum load. It was because the stiffness and the strength increased thanks to the composite effect of the deck plate and the concrete. Maximum live load ranged between 6.2 and 9.5 kN/m^2, which was three times as large as the live load.

Table 5. Consideration Load List

Dead Load (kN/m²)	Concrete	4.68
	Deck Plate	0.21
	Fnishing Material	0.88
	Total	5.77
Live Load (kN/m²)	2	
Total Force (kN)	Coefficient	34.7
	Usage	26.6

Table 4. Composite Degree Evaluation Result

	FC01	FC02	FC02	FC04	FC05
M_{fsc} (kN·M)	186.5	186.5	255.4	255.4	255.4
M_{nsc} (kN·M)	122.14	122.14	202.71	202.71	202.71
M_c (kN·M)	92.9	92.9	171.3	171.3	171.3
M_u (kN·M)	227	181.7	244.3	258.4	248.9
M_u / M_{fsc}	1.22	0.97	0.96	1.01	0.97
M_u / M_{nsc}	1.86	1.49	1.21	1.27	1.23
M_u / M_c	2.44	1.96	1.43	1.51	1.45

M_c: Moment of Concrete Slab except Deck Plate

Table 6. Load Verification and Maximum Live Load

	FC01	FC02	FC03	FC04	FC05
δ_{SL}	13.53	13.53	9.82	8.82	8.82
δ_{SL}/δ_{LMT}	0.54	0.54	0.39	0.35	0.35
$P_{SL}/P_{\max}$	0.26	0.33	0.24	0.23	0.23
$w_{LL,\max}$	6.2	5.8	8.4	9.2	9.5
$P_{LL,\max}/P_{\max}$	0.43	0.52	0.49	0.49	0.5

δ_{SL} : Deflection by Usage Load (mm)

δ_{LMT} : Deflection Limitation (L/300) (mm)

P_{FL} : Coefficient Load (kN)

$w_{LL,max}$: Maximum Live Strength (MPa)

$P_{LL,max}$: Strength by $w_{LL,max}$ (kN)

4.3. Composite effect and steel ratio

Figure 15 (a) shows the load - displacement relationships of specimen FC02 obtained from the formula and the test. Since the two are similar to each other, it is deduced that the knee of the test curve indicates the yield of the tendon. As shown in Figure 15 (b), the knee of the test curve of specimen FC03 which had an additional Rebar also indicates the yield of the tendon. But, specimen FC02 whose steel ratio was less than maximum steel ratio showed ductile behavior, while specimen FC03 which has over steel ratio showed brittle behavior.

TAs shown in Table 7, the steel ratio of specimen FC02 and specimen FC03 is 0.003911 and 0.007822, respectively. Steel ratio for tension-dominated cross-sections is 0.015952 if deck plates are not taken into consideration. Based on the ratio, both of the specimens are considered to have tension-dominated cross-sections. However, steel ratio for tension-dominated cross-sections with the composite effect of the concrete and the deck plates taken into consideration is 0.00661. Based on the ratio, the cross-sections of specimen FC03 are considered to be compression-dominated. Therefore, the tendon of specimen

Table 7. Rebar Ratio Comparison

	FC02	FC03
ρ_{sr}	0.003911	0.007822
$\rho_{sr,\,rc,\,\max}$	0.015952	
$\rho_{sr,\,sc,\,\max}$	0.00661	
$\rho_{sr,\,rc,\,\max}/\rho_{sr,\,sc,\,\max}$	0.414	

$\rho_{sr,\,rc,\,max}$: Maximum Rebar Ratio except Deck Plate

$\rho_{sr,\,sc,\,max}$: Maximum Rebar Ratio of Composed Deck Plate

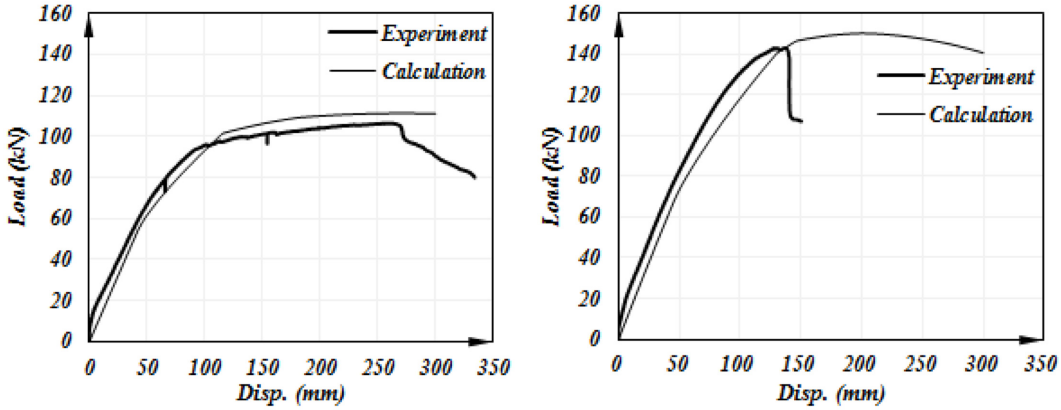
FC02 yielded before the compressive failure strain of the concrete (ε_{cu}) was reached. In specimen FC03, the concrete failed first and then the tendon yielded. It means that the load capacity of the slab decreased rapidly at the yield point of the tendon. Therefore, it is required to decrease steel ratio for complete composite slabs.

4.4. Effect of Pre-tension on Load Capacity and Ductility

Tendons are installed for introducing pre-tension. The deformation of the tendons evolves in three stages: 1) Deformation at the early stage of introducing pre-tension, 2) Deformation upon concrete casting and 3) Deformation while dealing with load after concrete hardening. Table 8 shows comparison between specimen FC01 without pre-tension and specimen FC02 with a pre-tension of 93 kN (188 MPa). Pre-tension introduced to the specimen

Table 8. Relationship between Tensional Load and Maximum Load

	FC01	FC02
ρ_{sr}	0.003911	0.003911
$F_{ps}(MPa)$	0	188
F_{re}/F_u	1	0.69
M_u (kN·M)	227	181.7
$M_u/M_{u,FC01}$	1	0.8
δ_f/δ_u	5.50	6.53



(a) FC02 (b) FC03

Fig. 15. Comparison of Structural Behavior according to Rebar Ratio. (FC02, FC03)

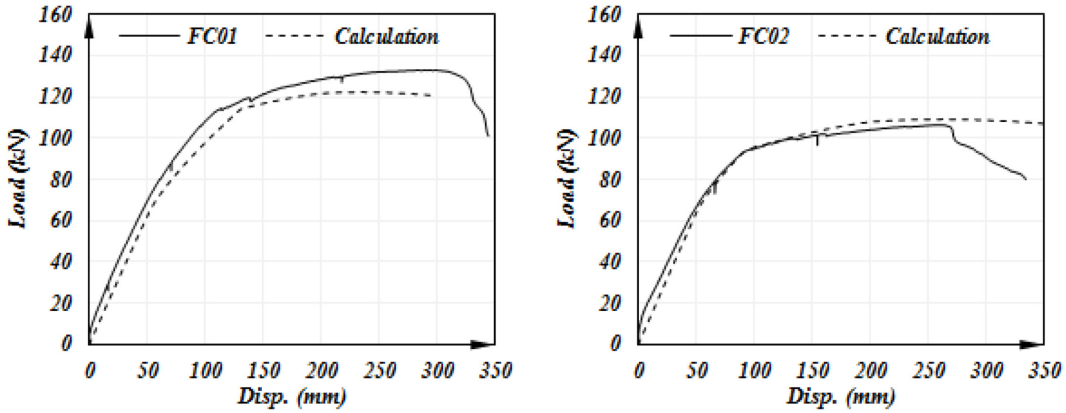


Fig. 16. Effect of Tension to Maximum Load and Ductility.

was approximately 30% of the tendon's yield strength and caused the maximum load capacity of the specimen to decrease by 20%.

As the graphs of Figure 16 show, load - displacement relationships obtained from estimation and the test were similar to each other in both specimen FC01 and specimen FC02. The knees of the theoretical curves were caused by the yield of the tendon. The test curves also indicate that the tendon yielded at the knees. Specimen FC01 yielded at a load of 113.84 kN and a strain of 117.72 mm. Specimen FC02 yielded at a load of 93.15 kN and a strain of 90.38 mm. The FC02 to FC01 ratio of strength at the yield of the tendon and the FC02 to FC01 ratio of strain were 0.82 and 0.81, respectively, which were similar to the maximum load capacity ratio shown in table 8. Therefore, it is deduced that how early the tendon yields exerts influence on the maximum load capacity of the member. If the tendon yields earlier, the slab shows ductile behavior because the displacement increases until the compressive failure strain of the concrete ($\varepsilon_{cu} = 0.003$) is reached. The ductility of specimen FC02 was greater than that of specimen FC01.

5. Conclusions

In a complete composite slab, the deck plate plays a role of a tensile member as well as a mold. It resists stress and exerts influence on the strain of the tendon. The tendon acts as a flexural reinforcing bar resisting tensile stress after concrete hardening and before loading and has positive effects on the floor structure. In order to verify these, structural tests were conducted on deep deck composite slab specimens with tendons for preloading. The conclusion of the tests and analyses is as follows.

- In all of the specimens, the strain of the concrete and the strain of the deck plate had a linear relationship until the yield load was reached. The ratio of maximum strength obtained from the test to estimated maximum strength approximated to 1, indicating the complete composite behavior of the deep deck composite slabs.
- The load capacity and deflection of the specimens were analyzed. The deflection limit was L/300 (25 mm). Deflection by working load was less than the limit in all of the specimens. The ratio of deflection by working load to deflection limit was between 0.35 and 0.55. The coefficient load was approximately 25% of the maximum load because the composite effect of the deck plate and the concrete increased the stiffness and strength. The available live load was calculated to be 6.2~9.5 kN/m^2, which was three times as large as the planned live load.
- Specimen FC02 whose steel ratio was 0.003911 showed ductile behavior, while specimenFC03 having a steel ratio of 0.0078222 showed brittle behavior. Maximum steel ratio with the deck plate taken into consideration was calculated to be 0.00661, which was a decrease of approximately 40% from the ratio calculated without considering the deck plate. Therefore, it is deemed that the cross-sectional area and yield strength of the deck plate should be taken into consideration when calculating steel ratio to be used in structural member design.
- Stress consumed to introduce pre-tension decreased the load capacity of the member after concrete hardening. The deformation of the tendon caused by the pre-tension induced the early yield of the tendon when the slab dealt with the load after concrete hardening and enabled the slab to display ductile behavior. The yield of the tendon is closely related to the yield of the whole member. The FC02 to FC01 ratio of load capacity at yield was similar to the FC02 to FC01 ratio of maximum load capacity. Although the maximum load capacity decreased by 20% due to pre-tension, the ductility increased by 1. It is deduced that pre-tension should be taken into consideration when the yield strength and the diameter of the tendon are determined.

References

Jeon, S. H., Kyung, J. H., Kim, Y. H., Choi, S. M., Yang, I. S., "Deflection Evaluation of the Constructing-load Carrying Capacity for Deep Decking Floor System Reinforced with Both Ends Cap Plates.", *Journal of Korean Society of Steel Construction*, 27(2), 155-167, doi: http://dx.doi.org/10.7781/kjoss.2015.27.2.155

Kim. C. W., Choi. S. M., Kang. D. A., Kim. D. K. (1997). "A Study on the Structural Behavior of the Composite Slabs Using the New Shaped Deck Plate", *Journal of Korean Society of Steel Construction*, 9(4), 589-600.

Kim. Y. S., Choi. S. M., Kim. D. K. (1999). "A Theoretical Study on the Structural Capacities and Fire Resistance Capacities for a Composite Slab Using Deck Plates", *Proceeding of Annual Conference of the Architectural Institute of Korea*, 19(2), 331-336.

Kim. Y. S., Kim. D. B., Nam. Y. S., Chae. H. S., Choi. S. M. (2011). "Development of Flexural Strength Program for a Full Composite Girders with Deck Plate", *Journal of the Korean Society of Advanced Composite Structures*, 2011(4), 37-40.

Kim, Y. H., Choi, S. M., LEE. S. H., "Construction Evaluation on the Form Deck System for Continuos Methods and Laterally Trussed Girder", *Journal of Korean Society of Hazard Mitigation*, 8(3), 67-78, doi: http://dx.doi.org/10.9798/KOSHAM.2015.15.6.35

Kim. Y. S., Shin. Y. S., Nam. Y. S., Chae. H. S., Choi. S. M. "Evaluation of Residual Strength of Preloaded Deep Deck Plate", *Journal of the Korean Society for Advanced Composite Structures*, 2011(4), 37-40.

Kwon. Y. H., Choi. S. M., Kang. D. A., Kim. D. K. (1997). "An Experimental Study on the Shear-Bond Strength for the Composite Slabs using Deck Plates", *Roceeding of Annual Conference of the Architectural Institute of Korea*, 17(2), 1,187-1,191.

Kwon. Y. K., Choi. S. M., Eom. C. H., Kang. D. A., Choi. O. C., Moon. T. S., Kim. K. S., Kim. D. J., Kim. D. K. (1996). "A Study on the Structural Behavior of the Composite Slabs using the Metal Form Deck Plate", *Journal of Korean Society of Steel Construction*, 8(2), 120-121.

Liu Peng (2014). "From Follows Fuction - The Composite Construction and Mixed Structures in Modern Tall Buildings", *International Journal of High-Rise Building*, 3(3), 191-198.

Park, K. Y., Jeon, S. H., Kim, Y. H., Choi, S. M., "A Study of Structural Performance of Self-Drilling Screw Connections", *Journal of Korean Society of Steel Construction*, 25(5), 543-553, doi: http://dx.doi.org/10.7781/kjoss.2013.25.5.543

Park, K. Y., Nam, Y. S., Kim, Y. H., Choi, S. M., "Improvement of Flexural Performance for Deep-Deck Plate using Cap Plate", *Journal of Korean Society of Steel Construction*, 25(5), 555-567, doi: http://dx.doi.org/10.7781/kjoss.2013.25.5.555